

Supplementary Information for Multimodal imaging of capsid and cargo reveals differential brain targeting and liver detargeting of systemically-administered AAVs

Jai Woong Seo¹, Javier Ajenjo¹, Bo Wu¹, Elise Robinson¹, Marina Nura Raie¹, James Wang¹, Spencer K. Tumbale¹, Pablo Buccino², David Alexander Anders², Bin Shen², Frezghi G. Habte³, Corinne Beinat¹, Michelle L. James¹, Samantha Taylor Reyes¹, Ravindra Kumar Sripriya⁴, Timothy F. Miles⁴, Jason T. Lee¹, Viviana Gradinaru⁴, Katherine W. Ferrara¹

¹Molecular Imaging Program at Stanford (MIPS), Department of Radiology, School of Medicine, Stanford University, Stanford, CA, USA.

²Stanford Cyclotron & Radiochemistry Facility (CRF), Department of Radiology, School of Medicine, Stanford University, Stanford, CA, USA.

³Stanford Center for Innovation in In vivo Imaging (SCi3), Department of Radiology, School of Medicine, Stanford University, Stanford, CA, USA.

⁴Division of Biology and Biological Engineering, California Institute of Technology, Pasadena, CA, USA.

Katherine W. Ferrara

Email: kwferrar@stanford.edu

This PDF file includes:

Supplementary Methods

The list of key material and reagents

Tables S1 to S3

Figures S1 to S7

Supplementary Methods

Assessment of *in vitro* transduction of CAP-B10 modified with Tz-NHS. To CAP-B10:CAG-mNG (5×10^{12} vg, 10 pmol) in 1x PBS (200 μ L), 0.1 M pH Na₂CO₃ solution (pH 9.1, 25 μ L) and 2 mM tetrazine NHS (1 μ L, 2 nmol) in anhydrous DMSO was added. After the incubation for 30 h at room temperature, the reaction mixture was quenched by adding 1x PBS (200 μ L, with 0.001% Pluronic F-68) and dialyzed in a mini-dialysis device (20 kDa molecular weight cut-off (MWCO)) in 500 mL 1x PBS (0.001% Pluronic F-68) overnight at 4 °C. The transduction of CAG-mNG by Tz-CAP-B10 and CAP-B10 was compared in HEK293T cells seeded at a density of 70% in a 24-well plate (3×10^4 cells/well) with 500 μ L of Dulbecco's Modified Eagle's medium (DMEM; Invitro- gen) supplemented with 10% fetal bovine serum (FBS; Invitrogen) and 1% penicillin–streptomycin (Invitrogen) (DMEMc). After incubation at 37 °C and 5% CO₂ for 24 h, media was aspirated and replaced with fresh DMEMc (250 μ L) at 1×10^5 vg/cell of Tz-CAP-B10 and CAP-B10. Cells were then incubated at 37 °C in a 5% CO₂ chamber for 24 h in virus-loaded media. Fluorescent microscopy images (**Fig. S1A**) were obtained, and cell media was replaced with fresh DMEMc (500 μ L). Cells were cultured for one additional day prior to collection. Media was aspirated and PBS (300 μ L) was added. Cells were trypsinized and centrifuged at 1500 rpm for 3 min at room temperature in 1.5 mL tubes and then washed with 1x PBS. Cells were washed for two cycles. In all, 4% paraformaldehyde (PFA) was added, and the pelleted cells were incubated for 10 min at room temperature. Fixed cells were centrifuged and PFA solution removed. Cells were washed with 1x PBS (500 μ L), centrifuged, and supernatant removed. This washing cycle was repeated two times. Afterwards, cells were resuspended in 1x PBS (500 μ L) and transferred to 5 mL flow cytometer tubes on ice. The frequency of green fluorescent cells was analyzed using a flow cytometer and FlowJo v10.1 software (**Fig. S1B**).

Details of PET Scanning. Animals were scanned for 30 minutes at 0, 4, and 21 hours p.i. Mice were anesthetized with 3.0% isoflurane in oxygen and maintained under 1.5–2.0% isoflurane during the imaging procedure. After the final imaging time point, mice were euthanized by Euthasol under deep isoflurane. Animals were then perfused with DMEM solution. Blood, brain, heart, lungs, liver, spleen, stomach, small intestine (SI), large intestine (LI), and muscle were harvested for biodistribution analysis. Radioactivity in each organ was measured with a gamma counter (Cobra Auto-Gamma Counter). Biodistribution of AAVs was presented as percent injected dose per gram of tissue (% ID/g).

PET/CT image analysis. For static image analysis of radiolabeled AAVs, the 30-min list mode data acquired at various time points (0, 4, and 21 hours) were reconstructed using 3D ordered-subset expectation maximization using maximum a posteriori (3D-OSEM/MAP) image reconstruction, corrected for isotope decay, detector normalization, and photon attenuation, but not scatter, and converted to units of %ID/g. For dynamic image analysis of [¹⁸F]DASA-23, the 30-min list mode data was segmented into 20 static time frames (15 x 8, 60 x 8, 300 x 4; seconds x frames) and processed as stated above. Quantitative PET image analysis was performed with Inveon Research Workplace (IRW) software after the coregistration of PET and CT images. Images were quantified by manually drawing regions of interest (ROI) in the left ventricle, brain, and liver as shown in the PET/CT images (**Fig. 1-3**). Tissue TACs were normalized to the percent injected dose per cubic centimeter (%ID/cc). For AAV PET image analyses, the cardiac ventricle was used to estimate the blood radioactivity concentration. To obtain the AAV uptake value without blood radioactivity, the vascular volume fraction (η , as a % of each organ), was determined from previous literature values^{60, 61} as 5% and 30% in the brain and liver, respectively. However, in this calculation we used 20% liver vascular volume fraction as 30% vascular volume fraction gives a negative radioactivity concentration at 5 min p.i. Therefore, the organ uptake value was calculated by the equation below. $R_{T,real}(t)$ is the AAV uptake value with radioactivity concentration units (%ID/cc) at the given time point. $R_T(t)$ is the target organ radioactivity (%ID/cc) from ROI analysis, and $R_B(t)$ is the blood radioactivity (%ID/cc) at the given time point⁶². Therefore, we have the relationship:

$$R_{T,real}(t) = R_T(t) - \eta R_B(t) \quad \text{(Equation 1)}$$

The Logan plot was then calculated for each AAV in the brain or liver at a given time after the administration of the AAV. $C_B(t)$ and $C_T(t)$ are the radioactivity concentration in the blood and target at a given time, and $IntC_B(t)$ and $IntC_T(t)$ are the accumulated radioactivity in the blood and target, respectively, from the time of injection to time (t). $IntC_T(t)/C_T(t)$ vs $IntC_B(t)/C_B(t)$ was then plotted. The slope and intercept of the plot was

then determined, and the distribution volume is estimated as the slope of a linear regression to the Logan plot. The slope is termed the distribution volume for historical reasons, although it is not technically a volume since an increase in the DV can be due to an increased number of binding sites within the same physical volume. For the AAVs described here, over the 30-min analysis period for the Logan plot, the AAVs are largely adherent to the epithelial cells as observed on optical imaging. Here, the distribution volume is proportional to the product of the receptor density and the ligand receptor association constant. Thus, in this case, the differences in the total distribution volume are interpreted as an increase in the number of bound AAVs due to differences in the ligand receptor association constant.

Tissue fixation. After excision of organs, the liver and brain were further fixed by immersion in 4% PFA at 4 °C. After overnight fixation at 4 °C, the liver and brain were sliced to 50 and 100 μm on a vibratome (Leica, VT-1000E) under 1xPBS. The floating tissue sections were transferred to a 24 well plate. Sliced tissues were immersed in blocking solution (5% donkey serum, 0.1% Saponin) for 1 hour, washed with antibody dilution solution (ADS, 1% donkey serum, 0.1% Saponin in 1xPBS) two times for 5 minutes, and incubated with primary antibody in ADS overnight at 4 °C. Tissues were rinsed three times in 1xPBS for 10 minutes, incubated with secondary antibody in ADS, rinsed again three times in 1xPBS for 5 minutes, and stained with DAPI (1/5000, 1xPBS, 0.1% saponin) for 20 minutes. Tissues were mounted with in ProLong glass antifade mountant (Thermo Fisher Scientific) on glass slides and cured overnight at room temperature. Tissues obtained at 3 weeks p.i. of AAVs for the assessment of transduction were stained with DAPI to visualize the tissue morphology and distinguish the central and portal vein. Mounted tissues are imaged with Leica TCS SP8 confocal microscope operated by LAS X 3.5.5. software (Leica). Whole liver and brain tissues were scanned with 20x lens and the scanned images were stitched to whole tissue image. The selected area was imaged with 60x lens and z-stack mode. Same sets of imaging data were acquired at the same laser power and gain level in each channel.

Fluorescence image processing and data analysis. Microscopic image process and ROI analyses were performed using LAS X (Leica). For Manders' overlap coefficient from Kupffer cells (CLEC4F, green) and Cy5-AAVs (red), twelve 20x images that obviously differentiated Kupffer cells and Cy5-AAVs from background were randomly selected from the scanned whole tissue image. The background and threshold of both channels (green and red) were adjusted, and images were binarized to represent Kupffer cell and Cy5-AAVs. Overlap coefficients were obtained from the overlay of binarized two channel images, calculated from a built-in extended tool of the Las X software (Leica). Mean fluorescence values were obtained by drawing ROIs provided in the Las X software (Leica).

To obtain the relative fluorescent intensity of Cy5-AAVs in cells in zone 1 (CV) over zone 3 (PV), more than five pairs of two ROIs, adjacent CV and PV pair as shown in **Fig. S7**, were drawn, and the mean fluorescent of zone 1 (CV) was divided by that of zone 3 (PV). The size of the round ROI was 0.03 mm² which covers a few layers of cells in each zone.

To obtain the mean fluorescent intensity of Cy5-AAVs within entire liver, 10 ROIs were randomly drawn on whole liver images, and the mean fluorescent values were obtained from Las X software (Leica). The fluorescent values were normalized over the number of fluorescent dyes per AAV particle injected to mice.

Quantitative polymerase chain reaction (qPCR) for counting vector genome. AAVs (5 μL) were incubated with freshly prepared DNase I solution (45 μL) for 30 minutes at 37 °C, which was further diluted 1/10 or 1/100 before qPCR analysis. TaqMan qPCR assay was performed with TaqMan Fast Advanced Master Mix and a set of TaqMan primers and probe identifying the WPRE sequence (assay ID: APZTHAW, 5'-GCATTGCCACCACCTGTCA (forward) and 5'-TCCGCCGTGGCAATAGG (reverse), and 5'-CTTTCCGGGACTTTTCG (FAM)) on CFX96 Touch real-time PCR detection system (Bio-Rad). Each AAV was assayed triplicate. The vector genome number was calculated by the standard curve obtained from the linearized CAG-mNeonGreen-WPRE or EF1A-PKM2-WPRE.

Western blot. The harvested brain tissue was transferred to 5 mL cryotubes, and immediately flash frozen with liquid nitrogen. After the tissue sample was transferred to ice, N-PER neuronal protein extraction reagent containing Halt protease inhibitor (Thermo Fisher Scientific) was added prior to tissue

homogenization. Homogenized tissue was centrifuged at 10,000 g for 10 min at 4 °C. After centrifugation, the supernatant was collected and characterized by a BCA assay to determine the concentration. The protein mixture was mixed with loading and reducing buffers following the manufacturers protocol and loaded into an SDS-PAGE gel (20 µg/well). After gel electrophoresis, the separated protein was transferred to a PVDF membrane (ThermoFisher Scientific) for Western blotting. PKM2 and β-actin were stained with a PKM2 monoclonal rabbit antibody (1:1000, Cell Signaling Technology) and rabbit anti-actin antibody (1:2000, Sigma Aldrich) as primary antibodies and Goat anti-rabbit IgG (H+L) antibody HRP conjugate (1:2000, Thermo Fisher Scientific) as the secondary antibody. Following antibody and chemiluminescence substrate (BioRed) incubation, protein bands were detected with a CCD detector (BioRad ChemiDoc XRS+) for further analysis.

The list of key materials and reagents.

Reagents	Source	Cat#
DNase I recombinant for AAV titer	Sigma Aldrich	4716728001
RNase-free DNase set	Qiagen	79254
ProLong glass antifade mountant	Thermo Fisher scientific	P36980
Superscript IV VILO Master Mix	Thermo Fisher scientific	11756050
TaqMan™ fast advanced master mix	Thermo Fisher scientific	4444557
TaqMan™ primers and probe (WPRE)	Thermo Fisher scientific	Assay ID: APZTHAW
TaqMan™ primers and probe (PKM2)	Thermo Fisher scientific	Hs00987261_g1
TaqMan™ primers and probe (TSPO)	Thermo Fisher scientific	Mm00437828_m1
TaqMan™ primers and probe (b-actin)	Thermo Fisher scientific	Mm02619580_g1
RNAprotect Tissue reagent	Qiagen	76104
N-Per neuronal protein extraction reagent	Thermo Fisher scientific	87792
Blocking buffer	Thermo Fisher scientific	37542
Normal donkey serum	Jackson ImmunoResearch	017-000-121
1xDPBS without Calcium and Magnesium	Corning	20-031-CV
10xDPBS without Calcium and Magnesium	Cytiva	SH30378.03
10xTBST	Cell Signaling Technology	9997S
Bolt MES SDS running buffer	Thermo Fisher scientific	B0002
Bolt LDS sample buffer	Thermo Fisher scientific	B0007
Bolt antioxidant	Thermo Fisher scientific	BT0005
Bolt sample reducing agent	Thermo Fisher scientific	B0009
Saponin	Sigma-Aldrich	47036-50G-F
Pluronic F-68	Thermo Fisher scientific	24040032
Ammonium citrate	Fluka	09833
Anhydrous DMSO	Biotium	90082
Tetrazine-PEG5-NHS ester	Click Chemistry tools	1143-10
Clarity™ Western ECL Substrate	Bio-Red	1705060
DAPI	Invitrogen	D3571
Cy5-TCO	Click Chemistry Tools	1089-1
4% PFA	Santa Cruz Biotechnology	
Devices	Source	Cat#
Mini-dialysis device (20k MWCO)	Thermo Fisher Scientific	88402
Amicon Ultra-15 Centrifugal filter unit 100kDa MWCO	EMD Millipore	UFC910024
Bolt 4-12% Bis-Tris plus gels	Thermo Fisher scientific	NW04120B
RNeasy Midi Kit for mRNA extraction	Qiagen	75144
iBlot 2 Transfer stacks PVDF mini	Thermo Fisher Scientific	IB24002
Instruments	Source	Cat#
Vibratome	Leica	VT-1000E
PET/CT scanner	Siemens	-
Confocal microscope	Leica	TCS SP8
Gel imaging CDC detector	Bio-Rad	ChemiDoc XRS+
Real-time PCR detection system	Bio-Rad	CFX96 Touch
Antibodies	Sources	Cat#; (RRID:AB)
Goat anti-mouse Clec4F antibody	R&D Systems	AF2784-SP
Donkey anti-Goat IgG (H+L) Cross-Adsorbed Secondary Antibody, Alexa Fluor 488	Thermo Fisher Scientific	A-11055 (AB_2534102)
Pkm2 XP® Rabbit mAb	Cell Signaling Technology	4053S (D78A4)
β-Actin Rabbit mAb	Cell Signaling Technology	4970S (13E5)
Tspo Rabbit mAb	Cell Signaling Technology	70358S (D1N7Z)
Goat anti-rabbit IgG(H+L) secondary antibody HRP	Thermo Fisher Scientific	31460 (AB_228341)

Table S1. AAV clearance half-lives following tail vein administration in mice.

Vector	Mouse strain	No. of mice	$t_{1/2}^a$ (h)	R^2	AUC_{brain}	AUC_{liver}
^{64}Cu -AAV9	C57BL/6	3	3.8	0.97	5.72	244
^{64}Cu -PHP.eB	C57BL/6	4	2.7	0.99	235	330
^{64}Cu -CAP-B10	C57BL/6	4	3.7	0.98	233	262

a. Adeno-associated virus clearance half-lives from blood, obtained from one-phase decay curve fit.

Table S2. Biodistribution of AAVs in organs (% ID/g) at 22 h.

	⁶⁴ Cu-AAV9 (n=3)		⁶⁴ Cu-PHP.eB (n=4)		⁶⁴ Cu-CAP-B10 (n=4)	
	mean	SEM	mean	SEM	mean	SEM
blood	6.7	0.7	3.5	0.1	5.3	0.4
brain	0.4	0.1	14.4	0.9	17.6	0.6
heart	2.3	0.5	2.3	0.1	2.3	0.3
lung	4.4	1.1	3.6	0.7	3.8	1.1
liver	20.0	0.8	23.5	1.4	22.9	1.9
spleen	10.7	0.5	24.6	1.5	32.0	2.0
stomach	2.9	0.3	2.3	0.3	2.7	0.5
SI	5.2	0.7	6.8	0.5	6.8	0.6
LI	4.9	0.4	8.7	0.4	8.6	0.7
kidneys	4.3	0.6	7.1	0.4	6.8	0.3
muscle	0.8	0.2	0.8	0.0	0.8	0.1

Table S3. AAVs, tags (⁶⁴Cu and Cy5) and reporter genes (eGFP, mNG, PKM2) used.

Experiment	Vector	Gene	Mouse strain	Data
⁶⁴ Cu-labeled AAV PET/CT	AAV9	<i>CMV-eGFP</i>	C57BL6	Fig. 1,3
	PHP.eB	<i>CAG-mNG-WPRE</i>	C57BL6	Fig. 1,3
	CAP-B10	<i>CAG-mNG-WPRE</i>	C57BL6	Fig. 1,3
¹⁸ F]DASA-23 PET/CT with PKM2 reporter gene	AAV9	<i>EF1A-PKM2-WPRE</i>	C57BL/6	Fig. 2
	PHP.eB	<i>EF1A-PKM2-WPRE</i>	C57BL/6	Fig. 2
Cy5-labeled AAV	AAV9	<i>CAG-mNG-WPRE</i>	C57BL6	Fig. 4,5
	PHP.eB	<i>CAG-mNG-WPRE</i>	C57BL6	Fig. 4,5
	CAP-B10	<i>CAG-mNG-WPRE</i>	C57BL6	Fig. 4,5

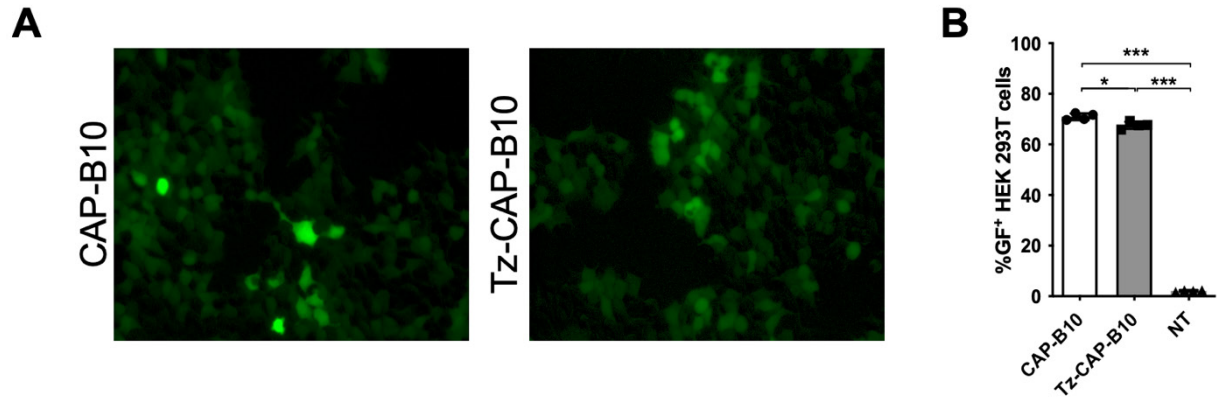
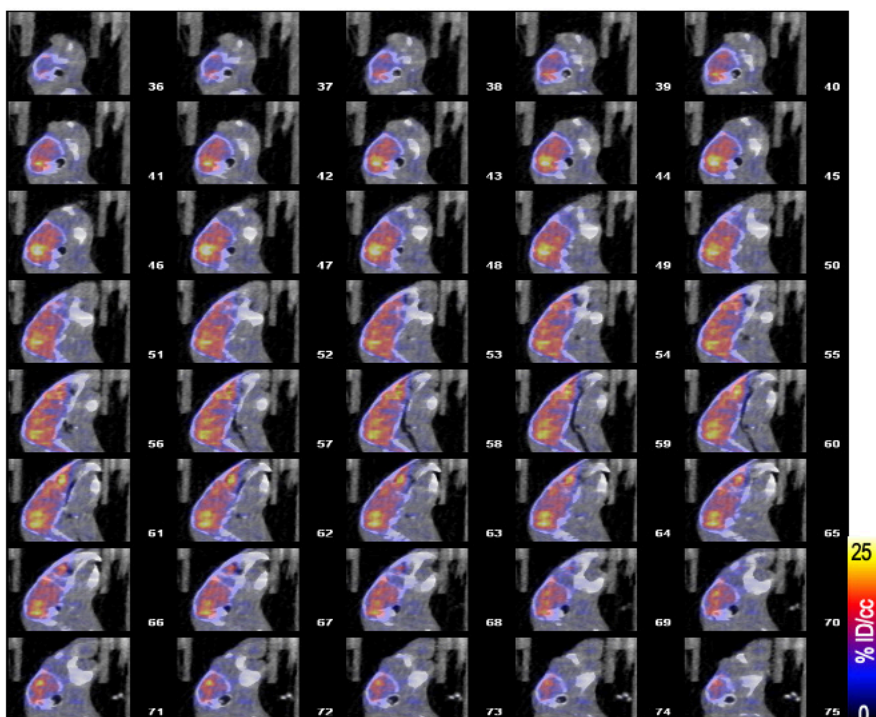


Figure S1. Transduction efficiency of tetrazine-conjugated CAP-B10. **A.** Fluorescent microscope images acquired at 24 h after incubation with CAP-B10 and tetrazine-conjugated CAP-B10 (Tz-CAP-B10). **B.** The percentage of green fluorescent cells from flow assay performed at 48 h after incubation of HEK 293T cells (MOI: 100,000). Data and error bars are presented as mean \pm SEM. Ordinary one-way ANOVA with Tukey's multiple comparison test was performed for the statistical analysis. * $P < 0.05$, *** $P < 0.001$.

^{64}Cu -PHP.eB



^{64}Cu -CAP-B10

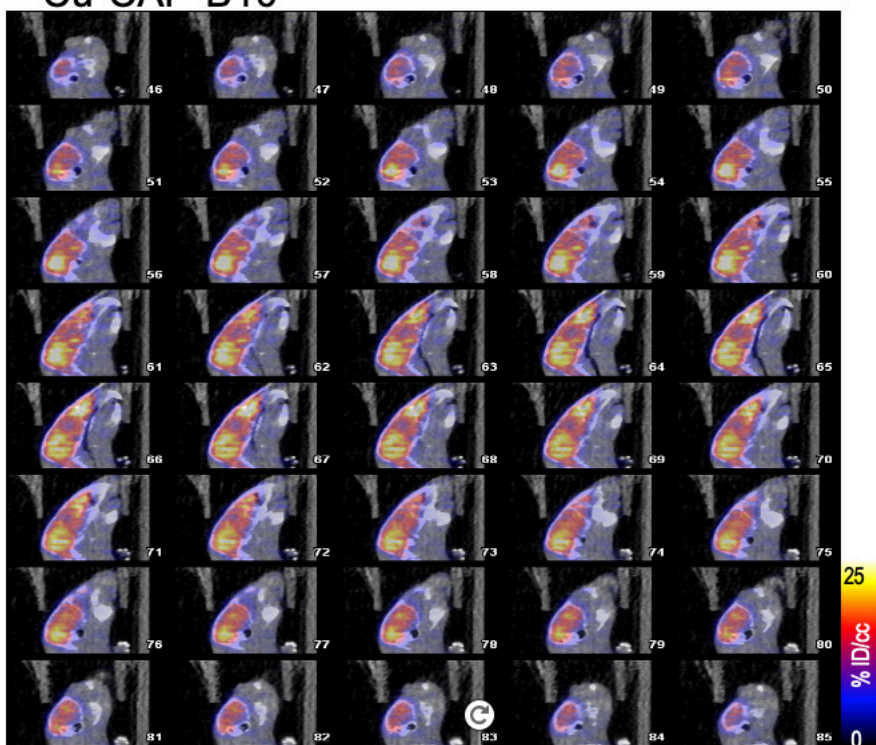


Figure S2. Representative brain PET/CT slice images at 21 hours p.i. of ^{64}Cu -PHP.eB and -CAP-B10.

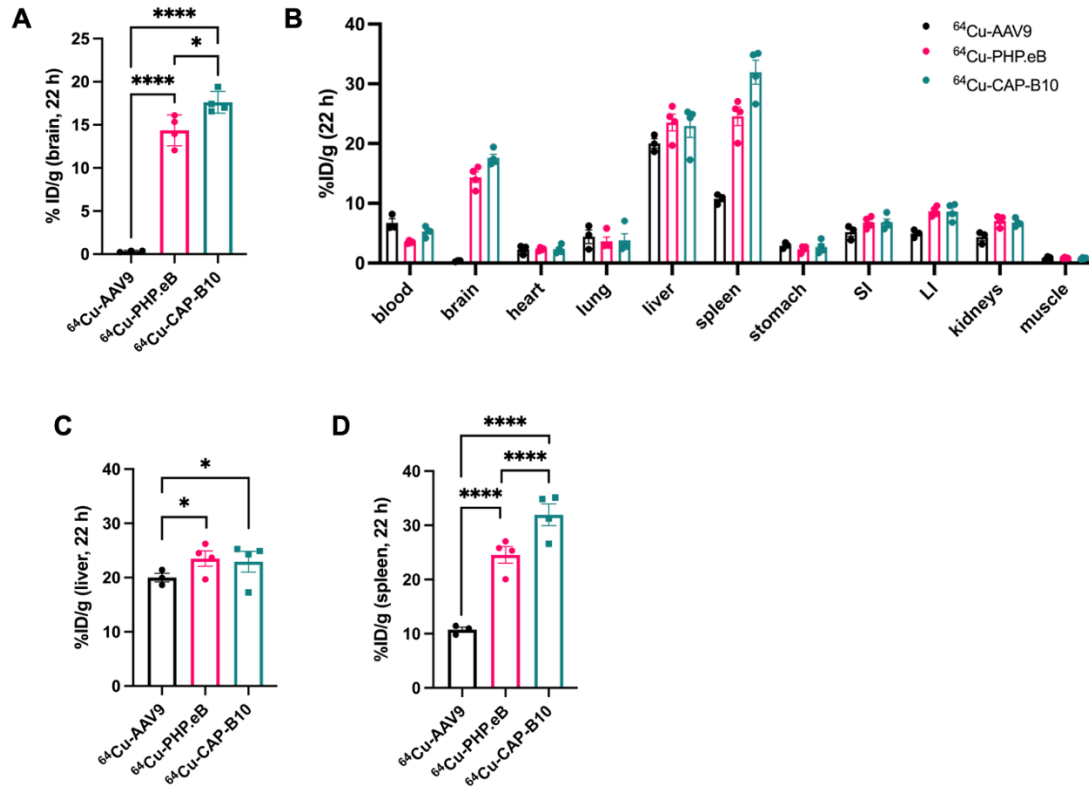


Figure S3. Biodistribution of engineered AAVs (PHP.eB and CAP-B10) and AAV9. A. Brain accumulation B. Whole body biodistribution. C-D. Liver and spleen accumulation of AAV9, PHP.eB and CAP-B10 in C57BL6 mice at 22 hours after injection. Data and error bars are presented as mean \pm SEM. Significance is tested with ordinary two-way ANOVA with Tukey's multiple comparisons test, with individual variance computed for each comparison. *P < 0.05, **** P < 0.0001. The percent injected dose per gram (%ID/g) is calculated from the biodistribution.

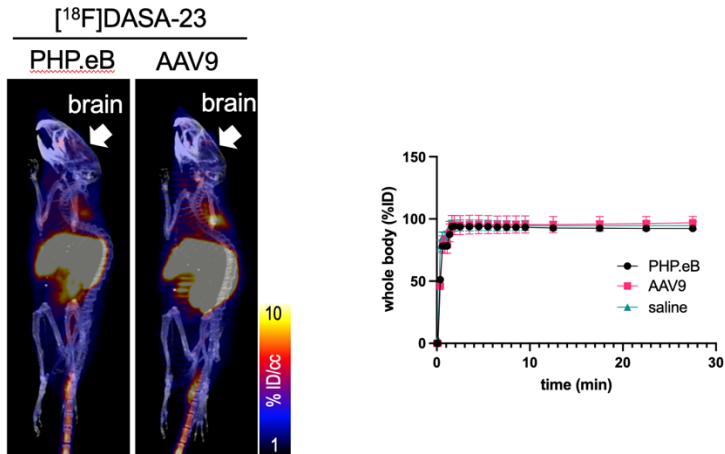


Figure S4. Representative maximum intensity projected (MIP) PET/CT images at 25-30 min after the tail vein administration of [¹⁸F]DASA-23 (left) and time-activity curve of [¹⁸F]DASA-23 clearance (right). Images were acquired at 3 weeks after systemic administration of AAV9- and PHP.eB packaging EF1A-PKM2 transgene.

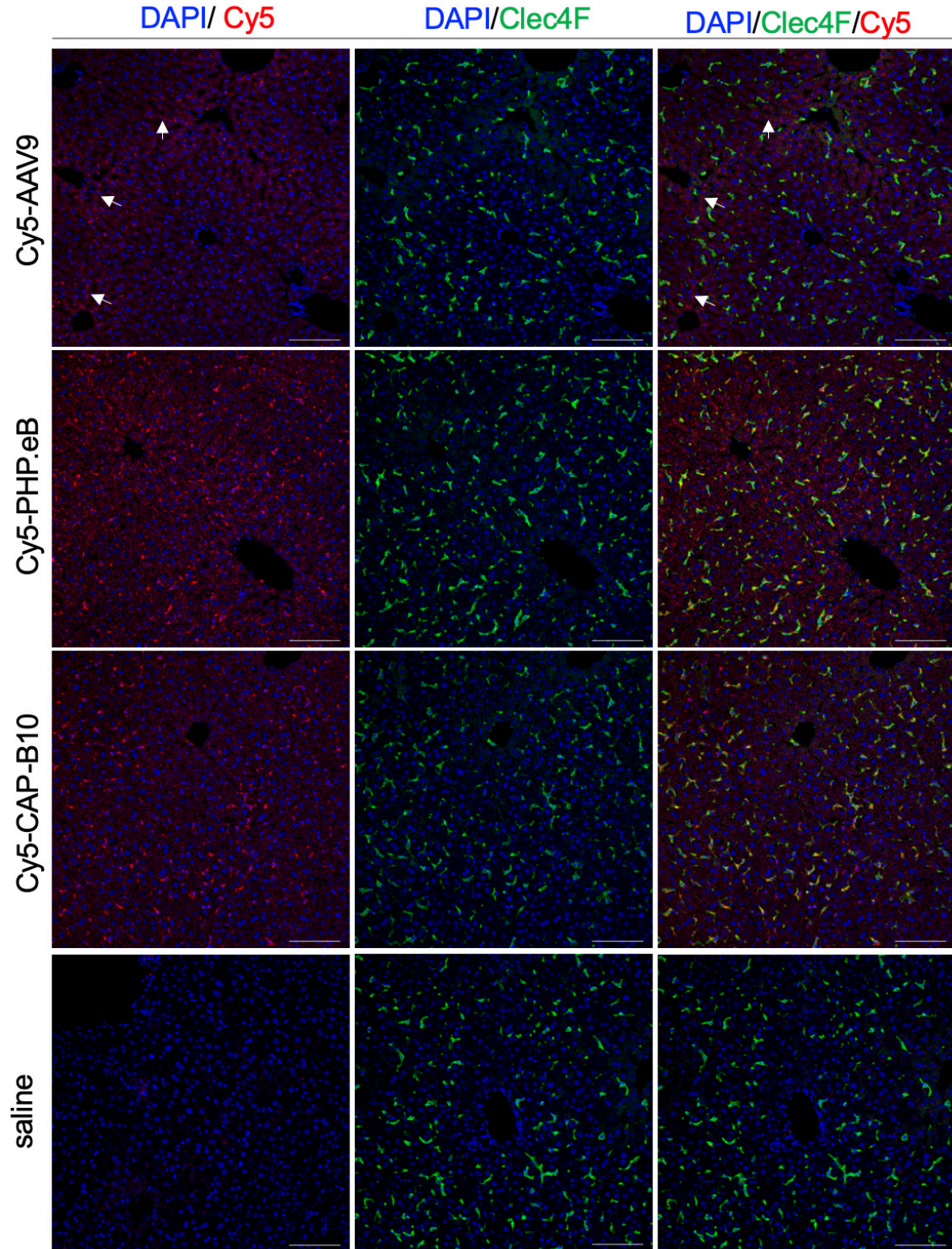


Figure S5. Representative FMI of mice liver sections in **Fig. 4C** and negative control (saline). Liver tissues were stained with Clec4F (green) for Kupffer cell and DAPI for nucleus (blue). Red channel (left) represents the presence of Cy5-labeled viral particles. White arrows indicate Cy5-AAVs in hepatocytes. Scale bar: 0.1 μm .

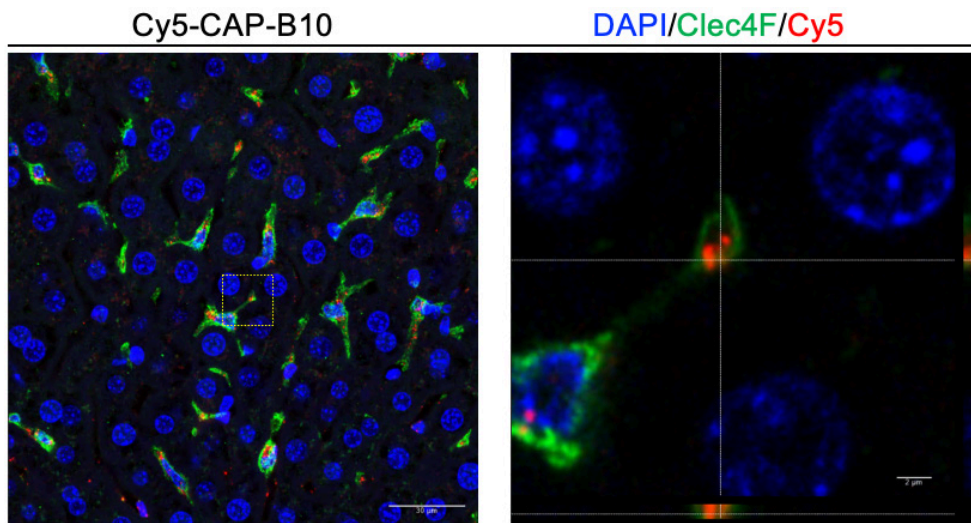


Figure S6. Z-section image of Cy5-CAP-B10 (left) and magnified region of square (yellow) from left image. Cy5-CAP-B10 (red) is on the surface and cytoplasm of Kupffer cell (Clec4F). Scale bar: 20 μm (left), 2 μm (right)

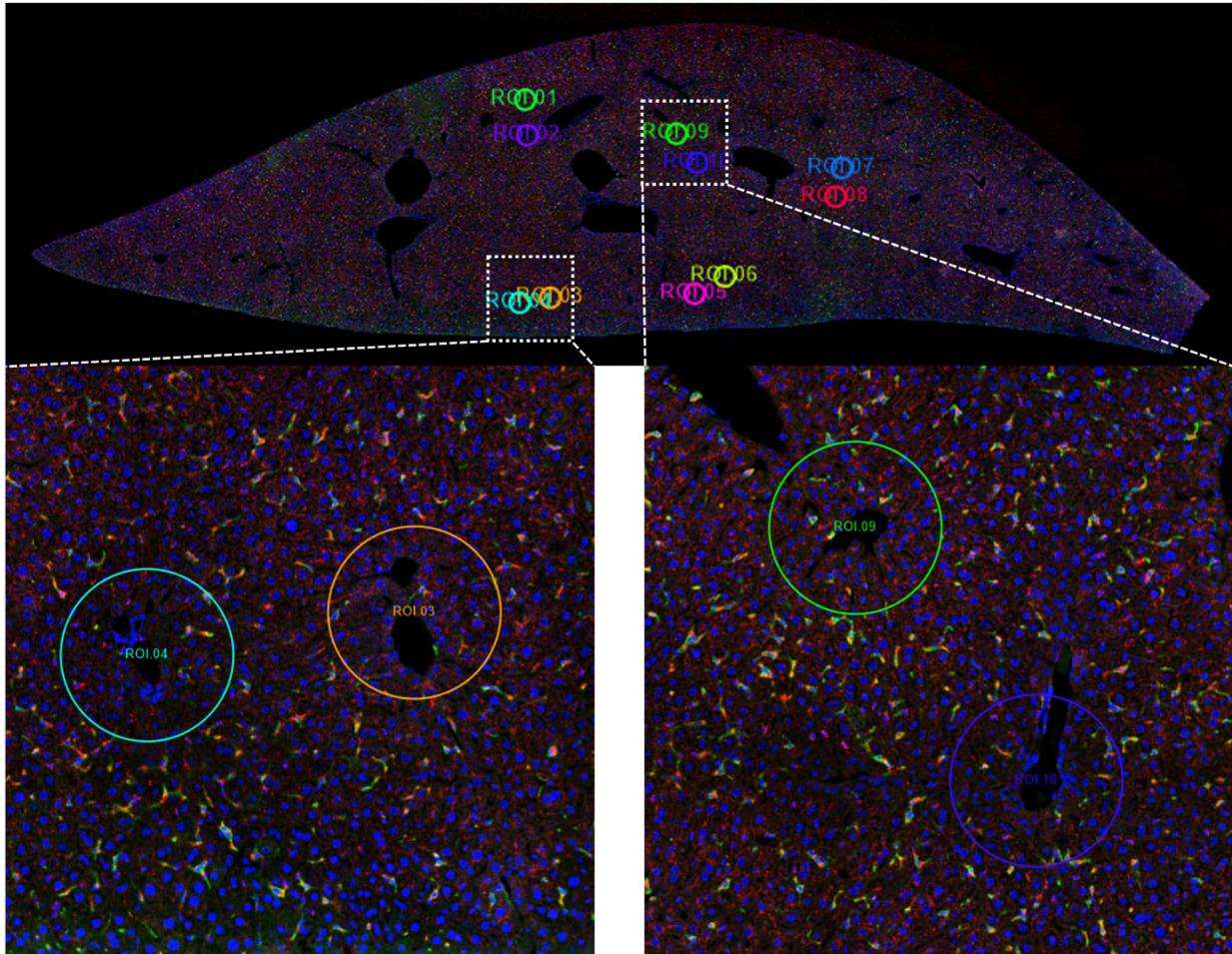


Figure S7. Representative FMI employed in the calculation of the relative fluorescent intensity of cells in zone 1 (CV) and zone 3 (PV) in liver tissue. Adjacent ROIs of zone 1 and zone 3 were drawn and their mean fluorescent intensity was calculated.